Available online at www.sciencedirect.com
SCIENCE DIRECT®
Journal of Power Sources 133 (2004) 302–311
JOURNAL OF POWER SOURCES
www.elsevier.com/locate/jpowsour

Preparation and characterization of $Ppy/Al_2O_3/Al$ used as a solid-state capacitor

Ming-Liao Tsai [a,*], Pei-Jiun Chen [b], Jing-Shan Do [b]

[a] *Department of Chemical Engineering, National Chin Yi Institute of Technology, Taiping City, Thichung County 411, Taiwan, ROC*
[b] *Department of Chemical Engineering, Tunghai University Thichung 407, Taiwan, ROC*

Received 5 November 2003; accepted 4 February 2004

Available online 10 April 2004

Abstract

The characteristics of a solid-state capacitor based on Ppy (polypyrrole)/Al_2O_3/Al prepared by the constant-current method are investigated. The surface composition of aluminum (Al) foil analyzed to by electron spectroscopy for chemical analysis (ESCA) is found to be AlO_2^- when the native oxide on the Al foil is etched by 0.1 M NaOH. Three stages are defined from the relationship between the potential and the electrolysis time in simultaneously preparing the dielectric layer (Al_2O_3) and the conducting polymer (Ppy) on Al foil etched with 0.1 M NaOH. The experimental results indicate that only stage one, i.e. the formation of Al_2O_3, occurs in the preparation of $Ppy/Al_2O_3/Al$ at a current density greater than 0.9 mA cm^{-2}. A higher concentration of pyrrole enhances the nucleation of Ppy within the pores of Al_2O_3 such that the period of the first stage decrease and the second stage of the propagation of Ppy is increased. The leakage current of $Ppy/Al_2O_3/Al$ rises from 0.009 to 0.405 μA cm^{-2} with increase in the concentration of pyrrole in preparing $Ppy/Al_2O_3/Al$ from 0.05 to 0.15 M. Raising the cut-off potential for preparing $Ppy/Al_2O_3/Al$ from 20 to 60 V increases the thickness of Al_2O_3 and lowers the capacity of $Ppy/Al_2O_3/Al$ from 478.5 to 174.2 nF cm^{-2}.

Keywords: Polypyrrole; Aluminum solid-state capacitor; Aluminum oxides; Dodecyl benzylsulfonic acid

1. Introduction

Microsystems, such as microsensors, are devices and complex functional units based on various microtechniques. It is very important to design a suitable power supply system to meet the requirements of microsystems. This includes consideration of the energy consumption, and the provision of continuous and pulse currents. The continuous current required for a microsystem can be supplied by microbatteries, such as thin-film lithuim batteries [1–6] and other thick-film batteries [7,8]. Microcapacitors can be designed and fabricated in the circuits of microsystems to meet the requirement of pulse current. Solid-state capacitors, instead of liquid electrolyte capacitors, are suitable for assembly in microsystems through the use of microfabrication technologies.

Recently, solid-state electrolytic capacitors with the characteristics of smaller size, higher capacitance, greater reliability and more safety have been developed based on MnO_2 [9–12], TCNQ (7,7,8,8-tetracyano-1,4-quinodimethane) [13–17]), or complex salts of organic semiconductor and conducting polymers [11,12,18–38]. The general requirements for a solid electrolyte for use in a solid electrolytic capacitor are considered to be [39]: (i) high conductivity; (ii) process ability to impregnate elements of capacitors; (iii) solid adhesion to dielectric films; (iv) heat-resistance and long life; (v) no reaction with metals used as dielectric films, or not causing deterioration of dielectric films; (vi) ability to restore dielectric films; (vii) stable temperature characteristics. Solid-state capacitors based on conducting polymers have been studied widely in recent years due to their good adhesion to dielectric films, good performance at high-frequency and temperature, and excellent stability.

Using polypyrrole (Ppy) as a counter electrode, solid electrolytic capacitors have been prepared based on tantalum [15,35,40–42], aluminum alloy [12], and aluminum [6,11,19–21,24–27,31,41]. The Ppy was prepared on Ta_2O_5/Ta by chemical oxidation at a very low temperature [35,43]. Excellent thermal and moisture stabilities have been found [25–27], for an aluminum solid electrolytic capacitor with Ppy electrochemically prepared on a pre-coating layer (MnO_2) as an eletroconducting-polymer electrolyte.

* Corresponding author. Tel.: +886-4-2392-450; fax: +886-4-2392-6617.
E-mail addresses: mltsai@chinyi.ncit.edu.tw (M.-L. Tsai), jsdo@mail.thu.edu.tw (J.-S. Do).

0378-7753/$ – see front matter © 2004 Published by Elsevier B.V.
doi:10.1016/j.jpowsour.2004.02.005

When Ppy was doped with tri-I-propylnaphthalenesulfonate (TIPNS), the conductivity of Ppy stemmed from the addition reaction of oxygen [26]. An aluminum solid electrolytic capacitor based on Ppy displayed better high-frequency performance and thermal stability on replacing MnO_2 with Ppy that was chemically synthesized on Al_2O_3 as a pre-coating layer [24].

The simultaneous formation of Ppy and aluminum oxide on an aluminum substrate has been reported [4,31,44–47]. Nevertheless, the capacitive characteristics of the simultaneous formation of Ppy/Al_2O_3/Al have been seldom reported [31]. This study focuses on the simultaneous preparation of an Al_2O_3 dielectric film and a Ppy solid polymer electrolyte on Al foil. The factors affecting the preparation of the Ppy/Al_2O_3/Al film and the characteristics of the resulting solid-state capacitor are investigated.

2. Experimental

2.1. Materials

All chemicals (e.g., pyrrole extra pure grade >99.99% ACROS), dodecyl benzylsulfonic acid (DBSA, pure grade, TCI), sodium hydroxide (GR grade >99%, MERCK), sodium hydrogen phosphate (pure grade, 99.1%, TEDIA), sodium dihydrogen phosphate (pure grade, SHOWA), HCl (GR grade, 37%, MERCK), and methyl alcohol (99.98%, TEDIA) were not further purified prior to usage.

2.2. Preparation of Ppy/Al_2O_3/Al film

The electrolyte for preparing Ppy/Al_2O_3/Al was prepared by mixing the desired amount of pyrrole monomer and DBSA in a suitable concentration of acid aqueous solution. Before electrolysis, the aluminum foil was impregnated in 0.1N NaOH for 1 h to remove the native oxide film on the surface. The aluminum foil after pretreatment was immediately placed in the electrolyte that had been purged with nitrogen to remove dissolved oxygen. Electrolysis was controlled at a constant-current by a d.c. power supply (Keithley 237).

2.3. Assembly and properties of solid-state capacitor

The assembly of the solid-state capacitor based on Ppy/Al_2O_3/Al is shown in Fig. 1. The capacitive characteristics of dissipation angle ($\tan\delta$), equivalent series resistance (ESR) and capacity (C_s), together with the leakage current (L_c) of the solid-state capacitor were measured by means of a LCR meter (Motech MT 4080A) and leakage current tester (Zentech CLC-203), respectively. The values of capacity (C_s) and $\tan\delta$ were measured at a frequency of 120 Hz, and the value of L_c was obtained at 100 kHz.

The surface morphologies of the aluminum foil substrate and the Ppy/Al_2O_3/Al were analyzed by scanning electron microscopy (SEM, JOEL, JSM-5400). The surface composition and state of the aluminum foil and chemical state were measured with electron spectroscopy for chemical analysis (ESCA) (PHI 1600).

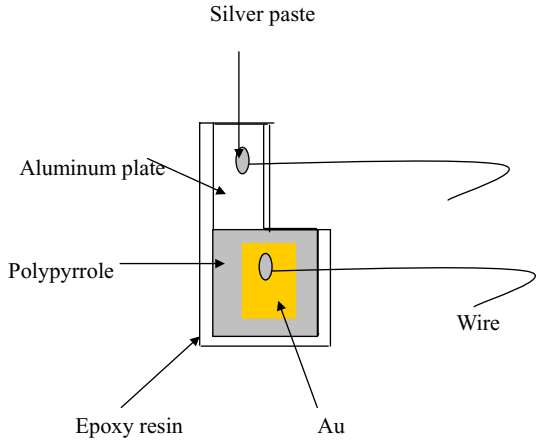

Fig. 1. Assembly of solid-state Ppy/Al_2O_3/Al capacitor.

3. Results and discussion

3.1. Surface composition of aluminum oxide/Al

The thin-film of native oxide must be etched and removed with 0.1N NaOH before the simultaneous preparation of the Ppy film and the aluminum oxide film on the surface of the aluminum foil. The binding energies of the untreated aluminum surfaces and those etched with 0.1N NaOH at 303 K for 1 h were analyzed with ESCA and illustrated in Fig. 2a and b. The binding energies of the aluminum foil surface etched with 0.1N NaOH and then anodized to form aluminum oxide in the 0.1 M DBSA solution are shown in Fig. 2c. The major elements on the surface of the aluminum are found to be Al, O and C.

The O:Al element ratio decreases from 4.9 for the untreated surface to 2.12 for the surface etched with 0.1 M NaOH. The binding energy of Al (2p) is shifted from the untreated surface value of 74.3 to 73.9 eV for the etched surface. In addition, the binding energy of O (1s) on the etched surface indicates that the composition of this surface is AlO_2^-. A similar result is obtained for Al treated with an aqueous solution of high pH [48]. When the etched surface is anodized to form an oxide film in DBSA aqueous solution, the composition of the resulting film is determined to be Al_2O_3 from the binding energies of Al (2p) and O (1s), which are 74.3 and 531.3 eV, respectively [49].

3.2. Preparation of Ppy/Al_2O_3/Al

Using aluminum pretreated with 0.1 M NaOH for 30 min as the working electrode, three stages are found from the relationship between potential and electrolysis time for prepar-

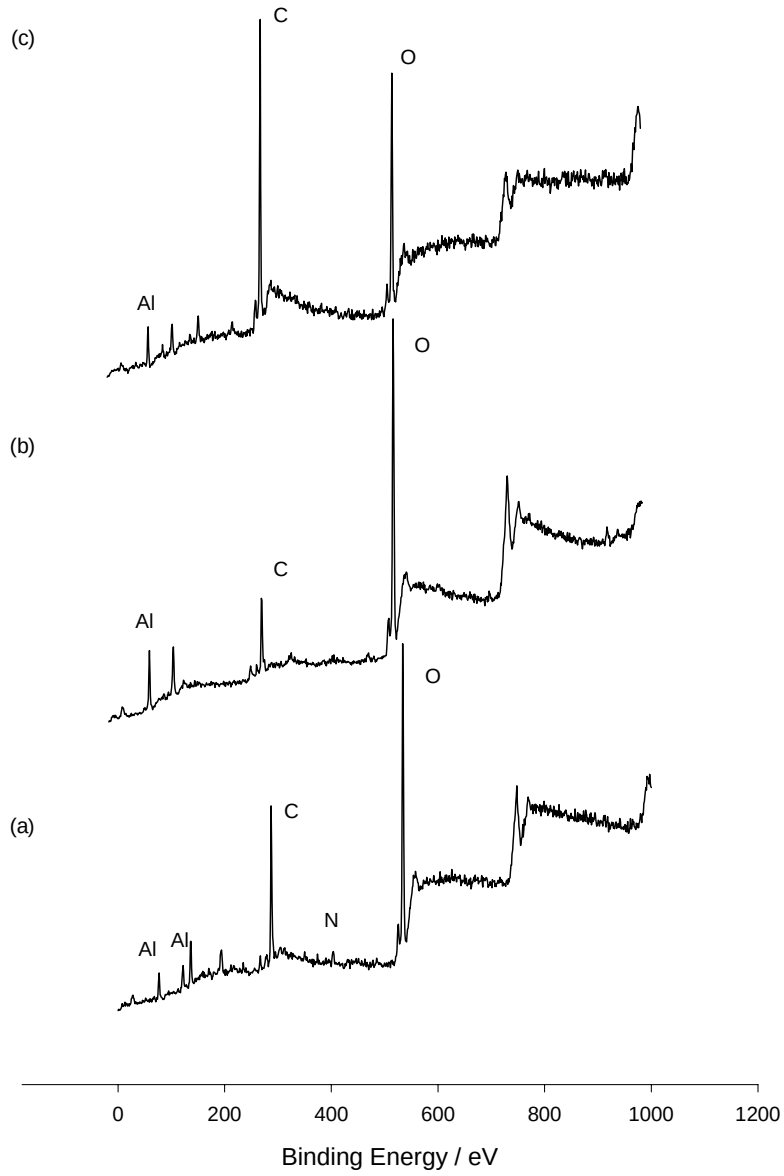

Fig. 2. ESCA spectra of surface of Al foil. (a) Raw Al plate; (b) pretreatment with 0.1 M NaOH at 30 °C for 1 h and (c) formation at 0.1 M DBSA with the cut-off potential of 60 V. Calibration for C (1s) at 284.6 eV.

ing Ppy/Al_2O_3/Al at 0.5 mA cm^{-2} (Fig. 3). During the first stage, the formation of aluminum oxide film is accompanied by the formation of nuclei of Ppy in the pores of the Al_2O_3. The sharp increase in potential from 0 to 9.36 V with increase in electrolysis time from 0 to 1.5 min is due mainly to the formation of aluminum oxides in the first stage. In this stage, the surfactant of DBSA acts as both a supporting electrolyte and a dopant, in the Ppy film, and assist penetration of pyrrole into the pores of the aluminum oxide film and the formation of nuclei on the aluminum substrate [4]. During the second stage, the main reaction on the anode is propagation of the conducting Ppy film based on the nuclei formed in the first stage. The high conductivity of the Ppy film causes a lower rate of increase in potential with time during this stage. The potential increases from 9.36 to 31.07 V with increase in electrolysis time from 1.5 to 40.0 min. Furthermore, during the last stage, the sharp increase in potential is due to over-oxidation of Ppy within the pores of the aluminum oxide, as well as a significant decrease in the conductivity of the Ppy/Al_2O_3 film located between the aluminum substrate and the aqueous electrolyte. The potential increases from 31.07 to 61.92 V with the increase in electrolysis time from 40.0 to 47.4 min, as illustrated in Fig. 3.

3.2.1. *Effect of current density*

Only the first stage is found in the relationship between potential and electrolysis time for current densities greater than 0.9 mA cm^{-2}, as shown in Fig. 4. The potential increases sharply from 0 to 56.3 V with increase in electrolysis time from 0 to 3.0 min for a current density of 0.9 mA cm^{-2}.

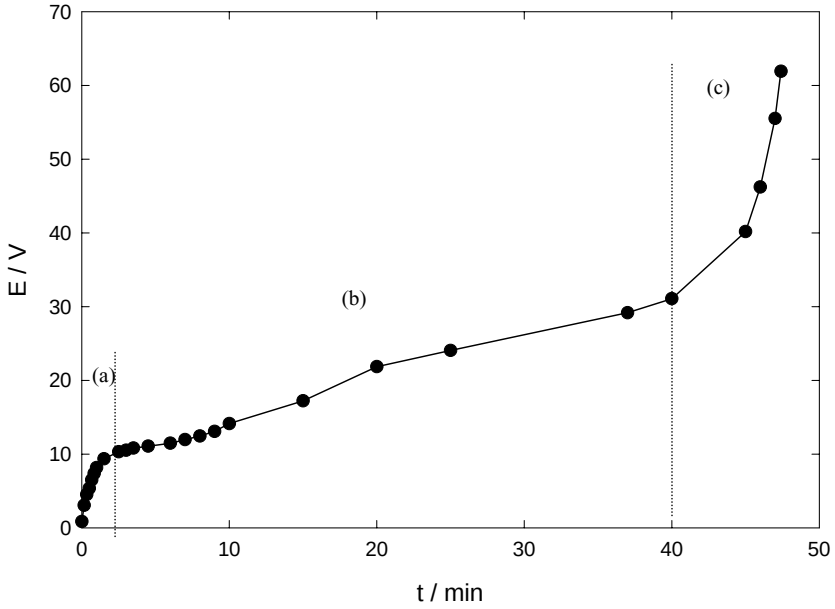

Fig. 3. Effect of electrolysis time on potential for preparing Ppy/Al_2O_3/Al. Area of Al foil = 1 cm × 1 cm, thickness of Al foil = 40 μm. Conditions for pre-treatment of Al foil: [NaOH] = 0.1 M, T = 30 °C, t = 0.5 h. Conditions for preparing Ppy/Al_2O_3/Al/Al: [pyrrole] = 0.1 M, [DBSA] = 0.1 M, initial pH = 1.3, T = 16 °C. Counter electrode: 2 cm × 3 cm stainless-steel plate. Current density = 0.5 mA cm^{-2}. (a) First stage; (b) second stage and (c) third stage.

The absence of the second stage at 0.9 mA cm^{-2} results in only a small amount of Ppy on the surface of the aluminum foil (Fig. 5a). The experimental results reveal that the rate of formation of Ppy nuclei within the pores of Al_2O_3 is much less than that for the formation of Al_2O_3. Hence, the second stage (the propagation of Ppy film) is not found for current densities greater than 0.9 mA cm^{-2}.

For a current density less than 0.75 mA cm^{-2}, the lower rate of formation of Al_2O_3 causes the Ppy film to grow on the surface of Al_2O_3 and the second stage is found from the relationship between potential and electrolysis time (Fig. 4). The Ppy film grows uniformly on the Al_2O_3/Al when a current density of 0.6 mA cm^{-2} is applied in the preparation of Ppy/Al_2O_3/Al, as shown in Fig. 5b. The period of the second stage in the preparation of Ppy/Al_2O_3/Al increases as the current density is lowered. The experimental results in Fig. 4 also reveal that the potential in the first stage increases from 6.65 to 16.4 V min^{-1} with increase in current density

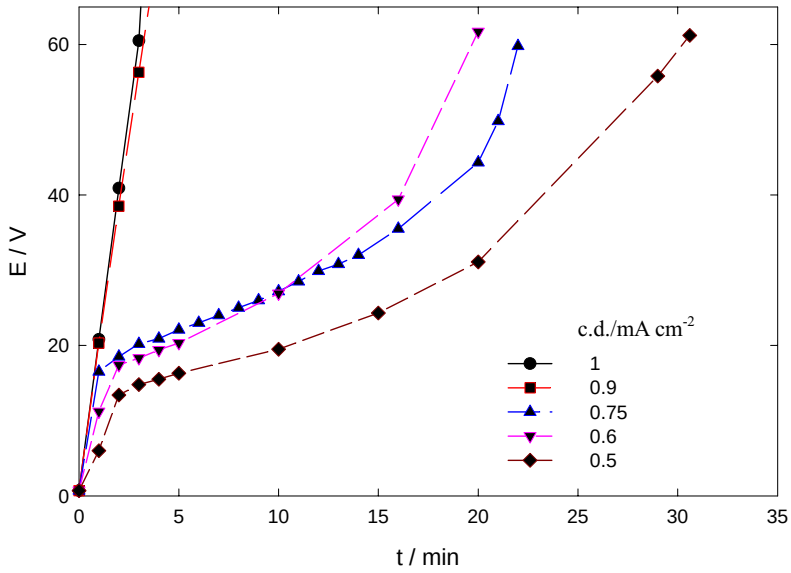

Fig. 4. Effect of electrolysis time on potential for preparing Ppy/Al_2O_3/Al film with various current densities. Area of Al foil = 1 cm × 1 cm, thickness of Al foil = 40 μm conditions for pre-treatment of Al foil: [NaOH] = 0.1 M, T = 30 °C, t = 0.5 h. Conditions for preparing Ppy/Al_2O_3/Al/Al: [pyrrole] = 0.1 M, [DBSA] = 0.1 M, initial pH = 1.3, T = 16 °C. Counter electrode: 2 cm × 3 cm stainless-steel plate.

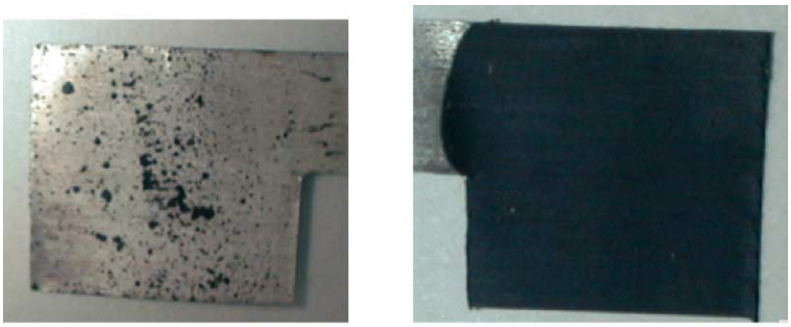

(a) (b)

Fig. 5. Photographs of Ppy/Al_2O_3/Al film prepared with various current densities. Area of Al foil = 1 cm × 1 cm, thickness of Al foil = 40 μm. Conditions for pre-treatment of Al foil: [NaOH] = 0.1 M, T = 30 °C, t = 1.0 h. Conditions for preparing Ppy/Al_2O_3/Al/Al: [pyrrole] = 0.1 M, [DBSA] = 0.1 M, initial pH = 1.3, T = 16 °C. Counter electrode: 2 cm × 3 cm stainless-steel plate. Current density: (a) 0.9 mA cm^{-2} and (b) 0.6 mA cm^{-2}.

from 0.5 to 0.75 mA cm^{-2}. The data indicate that electrolysis is favourable to the formation of Al_2O_3 when the current density used to prepare Ppy/Al_2O_3/Al is increased.

3.2.2. Surface composition of Ppy/Al_2O_3/Al

The surface composition is affected severely by the cut-off voltage applied in preparing Ppy/Al_2O_3/Al, as shown in the ESCA spectra (Fig. 6). The Al disappears and other elements such as C, N and S are simultaneously found on the surface when the potential for preparing Ppy/Al_2O_3/Al is greater than 15 V. As discussed above, the main reaction in the preparation of Ppy/Al_2O_3/Al is the formation of an Al_2O_3 film when the preparation is located in the first stage for potentials less than 15 V (Fig. 3). Therefore, the main elements on the surface found from the ESCA spectra are Al and O for potentials less than 15 V. On the other hand, when the potential is greater than 15 V, the preparation of Ppy/Al_2O_3/Al lies in the second stage (i.e., the propagation of Ppy film) and the surface of Al_2O_3/Al is covered by a Ppy film. Hence, the element Al disappears and elements N and S are found in the ESCA spectra (Fig. 6).

Furthermore, analysis of the ESCA diagram (Fig. 7) reveals that the binding energy of Al (2p) shifts from 74.5 to 74.3 eV and the binding energy of O (1s) shifts from 531.7 to 531.3 eV when the potential for preparing Ppy/Al_2O_3/Al is increased from 5 to 10 V. The shift in binding energies indicates that the state of aluminum oxide on the Al surface is changed from AlO_2^- to Al_2O_3.

3.2.3. Effect of concentration of pyrrole

Three stages in the relationship between potential and electrolysis time for preparing Ppy/Al_2O_3/Al are found in the presence of 0.1 M DBSA and various concentrations of pyrrole monomer (Fig. 8). The potential and the period of the first stage decreases from 22.45 V and 5.0 min to 10.65 V and 1.0 min, respectively, with increase in the concentration of pyrrole from 0.05 to 0.15 M. On increasing the concentration of pyrrole, the nucleation of Ppy within Al_2O_3 during the first stage increases and causes a decrease in the period and in the thickness of Al_2O_3. Hence, the potential in the first stage decreases with increase in the concentration of pyrrole. The period of the second stage increases from 31.5 to 105.0 min with increase in the concentration of pyrrole from 0.05 to 0.15 M, as indicated in Fig. 8.

3.2.4. Effect of temperature

At a temperature of 16 °C, first and second stages for preparing Ppy/Al_2O_3/Al are found in the ranges of 0 to 1.0 min and 1.0 to 95.0 min, respectively. The cut-off potential (60 V) is obtained for an electrolysis time of 104.8 min, as shown in Fig. 9. When the temperature is reduced to 6 °C, the second stage for preparing Ppy/Al_2O_3/Al commences after 1.0 min. The third stage is not observed until an electrolysis time of 140 min. Decrease in temperature increases the conductivity of Ppy and causes an increase in the propagation of Ppy during the second stage.

The relationship between potential and electrolysis time for various temperatures are illustrated in Fig. 10 for a cut-off potential of 20 V in the preparation of Ppy/Al_2O_3/Al. The period of the first stage increases from 1.0 to 3.0 min with reduction in temperature from 16 to −2 °C. As shown in Fig. 11, the potential versus electrolysis time is not affected by temperature in the absence of pyrrole monomer. The experimental results indicate that the effect of temperature on the formation rate of Al_2O_3 is insignificant. It is deduced that the longer period of the first stage in the preparation of Ppy/Al_2O_3/Al is mainly the results of a decrease in the nucleation rate of Ppy within the Al_2O_3 when the temperature is decreased. Furthermore, this extension of the first stage increases the thickness of the Al_2O_3 film, and raises the potential at the end of the stage.

3.3. Capacitive characteristics of Ppy/Al_2O_3/Al

3.3.1. Effect of cut-off potential in preparation of Ppy/Al_2O_3/Al

As discussed above, the potential for preparing Ppy/Al_2O_3/Al is mainly influenced by the Al_2O_3 barrier film. The thickness of the Al_2O_3 film has been shown to be proportional to the anodizing potential, i.e., 14 Å V^{-1} [50]. The

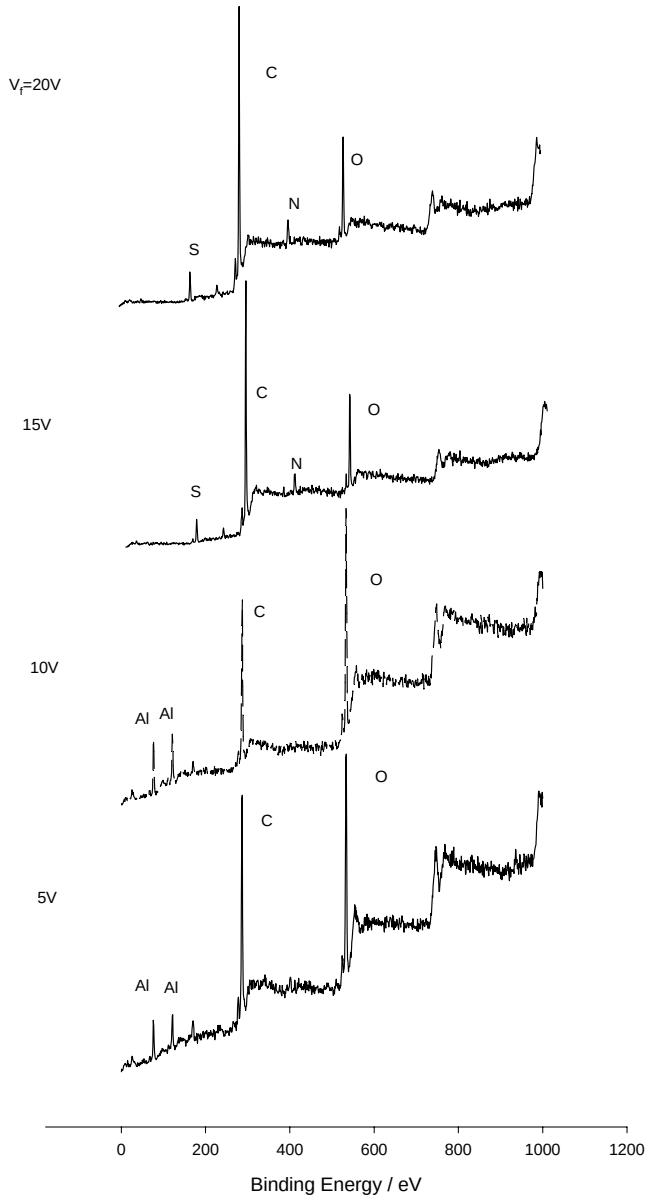

Fig. 6. Effect of cut-off potential for preparing Ppy/Al_2O_3/Al on ESCA spectra of surface of Ppy/Al_2O_3/Al. Area of Al foil = 1 cm × 1 cm, thickness of Al foil = 40 μm. Conditions for pre-treatment of Al foil: [NaOH] = 0.1 M, T = 30 °C, t = 1.0 h. Conditions for preparing Ppy/Al_2O_3/Al/Al: [pyrrole] = 0.1 M, [DBSA] = 0.1 M, initial pH = 1.3, T = 16 °C. Counter electrode: 2 cm × 3 cm stainless-steel plate. Current density = 0.6 mA cm^{-2}. Calibration for C (1s) at 284.6 eV.

capacity of the electrolytic capacitor is proportional to the reciprocal of the distance between the two electrodes, i.e., the thickness of the Al_2O_3 barrier layer. The capacity of Ppy/Al_2O_3/Al decreases from 478.5 to 174.2 nF cm^{-2} as the cut-off potential is taken from 20 to 60 V, as shown in Table 1 and Fig. 12. Increase of the Al_2O_3 barrier layer will result in a decrease of conductivity and leakage current between the two electrodes. The leakage current (L_c) falls from 0.892 to 0.032 μA cm^{-2} with increase in cut-off potential from 20 to 60 V (Table 1).

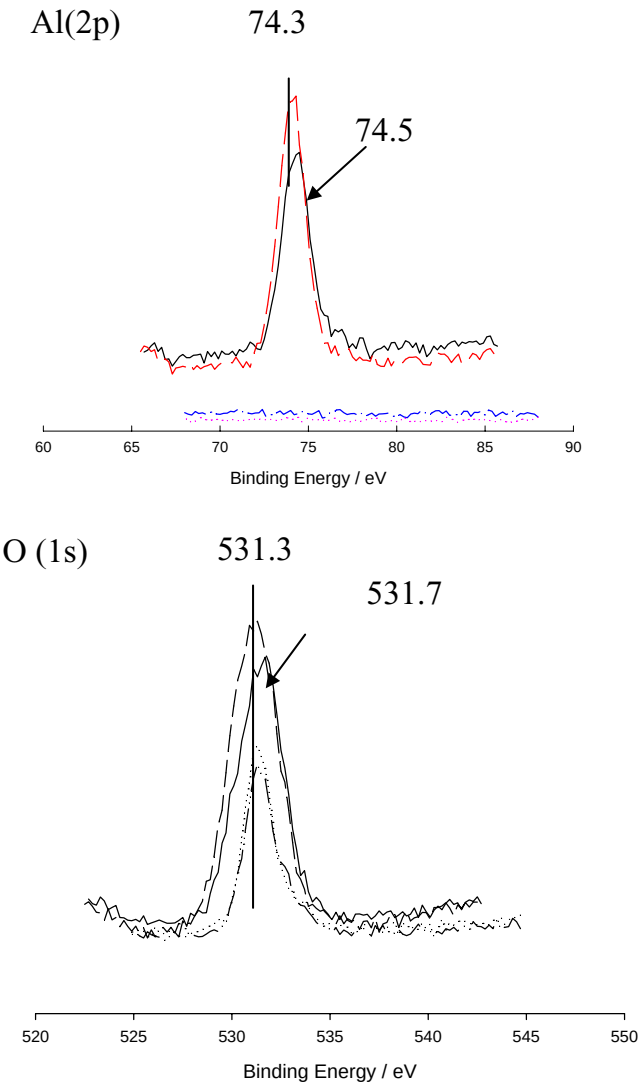

Fig. 7. ESCA spectra for Al (2p) and 0 (1s) of Ppy/Al_2O_3/Al film with various terminated potentials. Area of Al foil = 1 cm × 1 cm, thickness of Al foil = 40 μm. Conditions for pre-treatment of Al foil: [NaOH] = 0.1 M, T = 30 °C, t = 1.0 h. Conditions for preparing Ppy/Al_2O_3/Al/Al: [pyrrole] = 0.1 M, [DBSA] = 0.1 M, initial pH = 1.3, T = 16 °C. Counter electrode: 2 cm × 3 cm stainless-steel plate current density = 0.6 mA cm^{-2}. Calibration for C (1s) at 284.6 eV. Terminated potential: (— — —) 5 V; (– – –) 10 V; (- - -) 15 V; (. . .) 20 V.

Table 1
Effect of cut-off potential, concentration of pyrrole and temperature for preparing Ppy/Al_2O_3/Al on leakage current and capacity

V_f (V)	[Pyrrole] (M)	T (°C)	L_c (μA cm^{-2})	C_s (nF cm^{-2})
20	0.1	16	0.892	478.5
25	0.1	16	0.439	434.2
30	0.1	16	0.104	358.9
40	0.1	16	0.200	265.2
50	0.1	16	0.401	239.2
60	0.1	16	0.032	174.2
60	0.05	6	0.009	195.6
60	0.075	6	0.006	184.0
60	0.1	6	0.032	174.2
60	0.15	6	0.405	193.8
20	0.1	−2	0.07	468.4
20	0.1	6	0.472	522.9
20	0.1	16	0.892	448.5

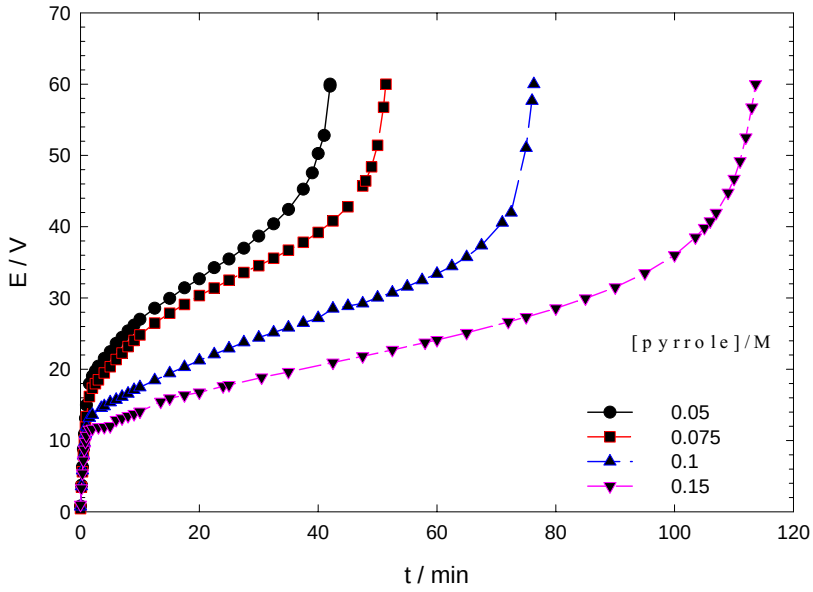

Fig. 8. Effect of electrolysis time on potential for various concentrations of pyrrole. Area of Al foil = 1 cm × 1 cm, thickness of Al foil = 40 μm. Conditions for pre-treatment of Al foil: [NaOH] = 0.1 M, T = 30 °C, t = 1.0 h. Conditions for preparing Ppy/Al_2O_3/Al/Al: [DBSA] = 0.1 M, initial pH = 1.3, T = 16 °C. Counter electrode: 2 cm × 3 cm stainless-steel plate. Current density = 0.6 mA cm^{-2}.

3.3.2. *Effect of concentration of pyrrole on preparation of Ppy/Al_2O_3/Al*

When the concentration of pyrrole for preparing Ppy/Al_2O_3/Al is increased from 0.05 to 0.15 M, and the cut-off potential and the temperature are set at 60 V and 6 °C, respectively, the leakage current rises from 0.009 to 0.405 μA cm^{-2}, and the capacity of Ppy/Al_2O_3/Al changes slightly (Fig. 13 and Table 1). Increasing the concentration of pyrrole results in longer period for Ppy propagation (second stage) and a greater thickness of Ppy (Fig. 8). The experimental results reveal that the capacity of Ppy/Al_2O_3/Al is determined by a very thin layer of Ppy that is closed to the Al_2O_3 barrier layer. Hence, the effect of the thickness of Ppy on capacity is insignificant. On the other hand, the dielectric property of the Al_2O_3 barrier may be affected by the concentration of pyrrole in the solution for

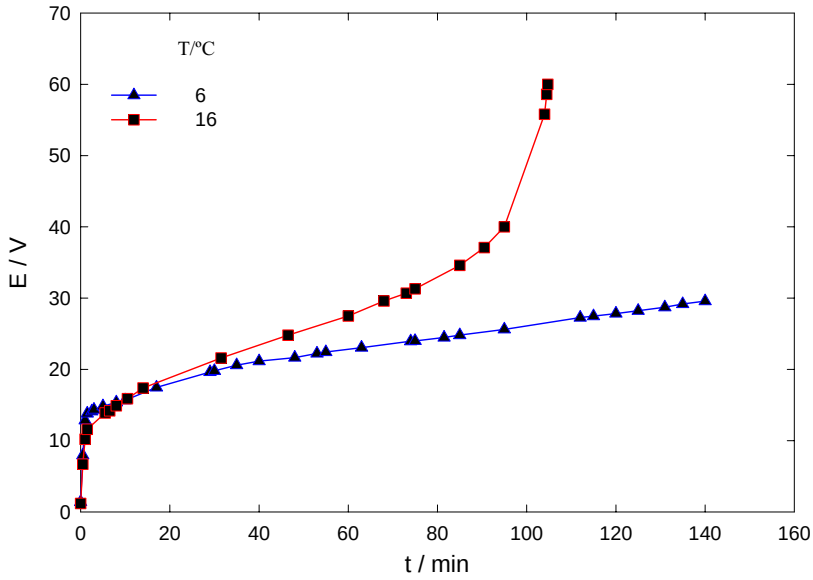

Fig. 9. Effect of electrolysis time on potential for various temperatures (cut-off voltage for preparing Ppy/Al_2O_3/Al of 60 V); Area of Al foil = 1 cm × 1 cm, thickness of Al foil = 40 μm. Conditions for pre-treatment of Al foil: [NaOH] = 0.1 M, T = 30 °C, t = 1.0 h. Conditions for preparing Ppy/Al_2O_3/Al/Al: [pyrrole] = 0.1 M, [DBSA] = 0.1 M, initial pH = 1. Counter electrode: 2 cm × 3 cm stainless-steel plate. Current density = 0.6 mA cm^{-2}.

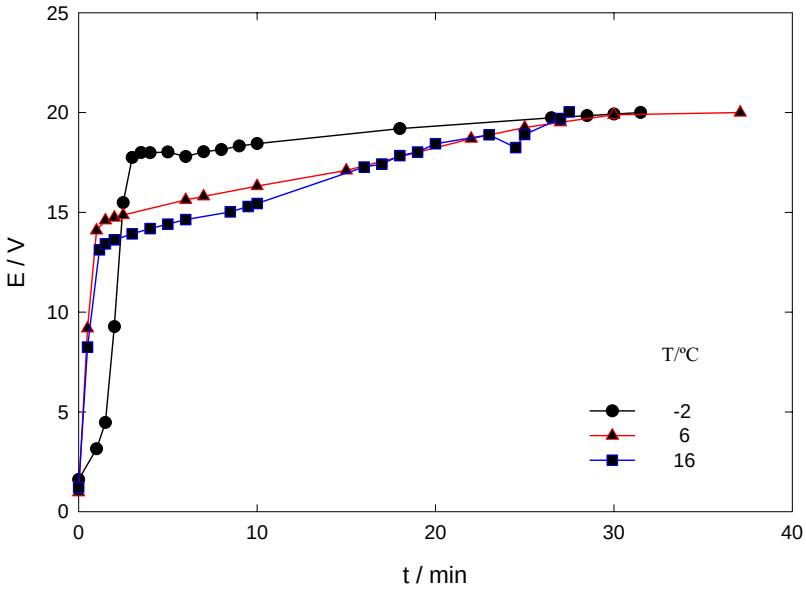

Fig. 10. Effect of electrolysis time on potential for various temperatures (cut-off voltage for preparing Ppy/Al_2O_3/Al of 20 V); area of Al foil = 1 cm × 1 cm, thickness of Al foil = 40 μm. Conditions for pre-treatment of Al foil: [NaOH] = 0.1 M, T = 30 °C, t = 1.0 h conditions for preparing Ppy/Al_2O_3/Al/Al: [pyrrole] = 0.1 M, [DBSA] = 0.1 M, initial pH = 1.3. Counter electrode: 2 cm × 3 cm stainless-steel plate. Current density = 0.6 mA cm^{-2}.

preparing Ppy/Al_2O_3/Al. Consequently, the leakage current of Ppy/Al_2O_3/Al increases with increase in the concentration of pyrrole.

3.3.3. *Effect of temperature on preparation of Ppy/Al_2O_3/Al*

On decreasing the temperature, both the period and the potential of the first stage for preparing Ppy/Al_2O_3/Al increase (Fig. 10). This behaviour may be due to the lower nucleation rate of Ppy within the pores of the Al_2O_3 during the first stage of Ppy/Al_2O_3/Al preparation. Therefore, a decrease in the amount of nuclei within the Al_2O_3 barrier layer induces an increase in the resistivity of the barrier layer when the temperature is decreased. By Contrast leakage current of Ppy/Al_2O_3/Al is decreased. As shown in Table 1, the leakage current decreases from 0.892 to 0.07 μA cm^{-2} with decrease in temperature from 16 to −2 °C. On the

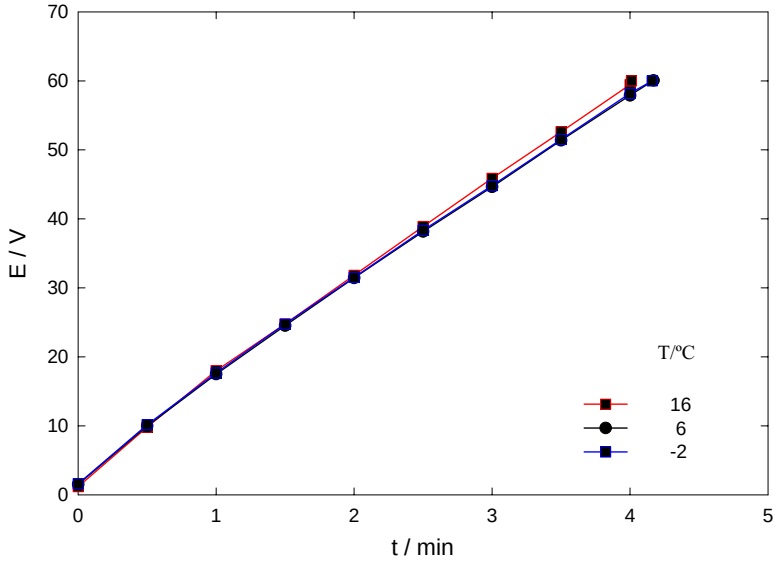

Fig. 11. Relationship of potential with time for formation of Al in absence of pyrrole. Area of Al foil = 1 cm × 1 cm, thickness of Al foil = 40 μm. Conditions for pretreatment of Al foil: [NaOH] = 0.1 M, T = 30 °C, t = 1.0 h. Conditions for preparing Al_2O_3/Al/Al: [DBSA] = 0.1 M, initial pH = 1.3. Counter electrode: 2 cm × 3 cm stainles-steel plate. Current density = 0.6 mA cm^{-2}.

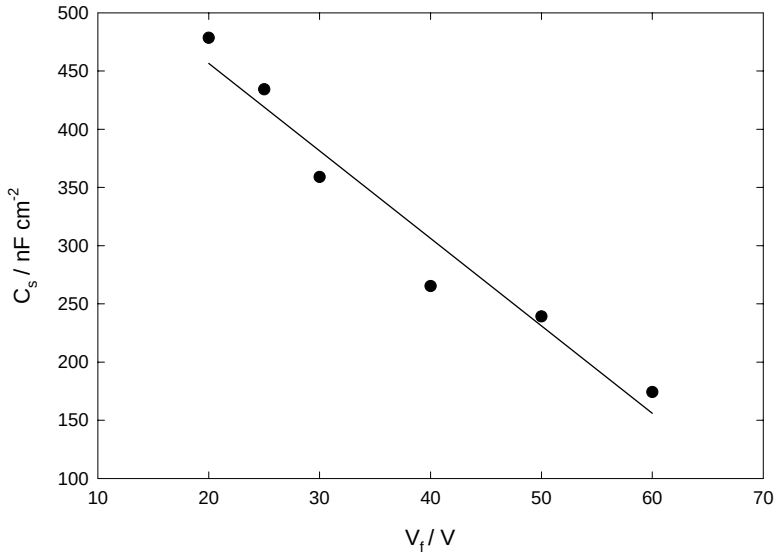

Fig. 12. Effect of terminated potential for preparing Ppy/Al_2O_3/Al on capacity. Area of Al foil = 1 × 1 cm, thickness of Al foil = 40 μm. Conditions for pre-treatment of Al foil: [NaOH] = 0.1 M, T = 30 °C, t = 1.0. Conditions for preparing Al_2O_3/Al/Al: [pyrrole] = 0.1 M, [DBSA] = 0.1 M, initial pH = 1.3. Counter electrode: 2 cm × 3 cm stainless-steel plate. Current density = 0.6 mA cm^{-2}.

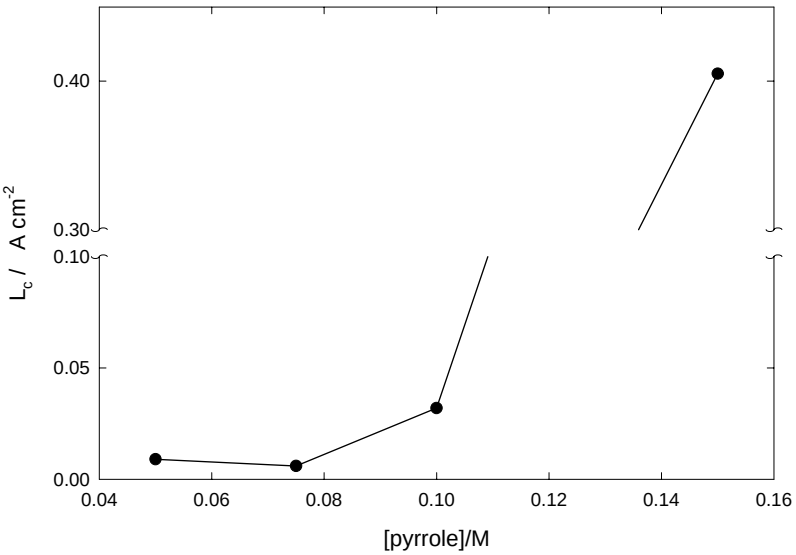

Fig. 13. Effect of concentration of pyrrole for preparing Ppy/Al_2O_3 on leakage current. Area of Al foil = 1 cm × 1 cm, thickness of Al foil = 40 μm. Conditions for pre-treatment of Al foil: [NaOH] = 0.1 M, T = 30 °C, t = 1.0 h. Conditions for preparing Al_2O_3/Al/Al: [DBSA] = 0.1 M, initial pH = 1.3. Counter electrode: 2 cm × 3 cm stainless-steel plate, current density = 0.6 mA cm^{-2}.

other hand, the capacity is only slightly affected by temperature.

4. Conclusions

Ppy and a Al_2O_3 barrier layer are prepared simultaneously on Al foil by the constant-current method. The surface composition of Al foil pretreated with 0.1 M NaOH aqueous solution and anodized in 0.1 M DBSA aqueous solution is analyzed by means of ESCA and found to be AlO_2^- and Al_2O_3. Three stages, namely the formation of Al_2O_3 and the nucleation of Ppy within the pores of Al_2O_3, the propagation of Ppy on the Al_2O_3 barrier layer and the over-oxidation of Ppy located in the pores of Al_2O_3, are found from the relationship of potential and the electrolysis time. When the current density for Ppy/Al_2O_3/Al preparation is greater than 0.9 mA cm^{-2}, the second stage is insignificant and very little of the Ppy film is found on the Al_2O_3 barrier layer. On increasing the concentration of pyrrole in the aqueous solution, the nucleation of Ppy within the Al_2O_3 during the first stage increases and causes a decrease in the period and the thickness of Al_2O_3 in the first stage, but increases the period of the second stage (the growth of Ppy on the Al_2O_3 barrier layer). Increasing the concentration of pyrrole for prepar-

ing Ppy/Al_2O_3/Al from 0.05 to 0.15 M leakage current from 0.009 to 0.405 $\mu A\,cm^{-2}$. The leakage current also decreases with decrease in the temperature for Ppy/Al_2O_3/Al preparation due to the lower nucleation rate of Ppy in the first stage. The effect of both the concentration of pyrrole and the temperature for Ppy/Al_2O_3/Al preparation on capacity is insignificant. On the other hand, the capacity of Ppy/Al_2O_3/Al is decreased markedly from 478.5 to 174.2 $nF\,cm^{-2}$ with increase of the cut-off potential for preparing Ppy/Al_2O_3/Al from 20 to 60 V.

Acknowledgements

The authors are grateful for financial support from Her Mei Electronic Co. Ltd. and the National Science Council of the Republic of China (NSC 91-2622-E-029-001-CC3), and for assistance from the Ministry of Education of the Republic of China (EX-91-E-FAO9-5-4), National Chin-Yi Institute of Technology and Tunghai University.

References

[1] J.B. Bates, N.J. Dudney, D.C. Lubben, G.R. Gruzalski, B.S. Kwak, X. Yu, R.A. Zuhr, J. Power Sources 54 (1995) 58–62.
[2] J.B. Bates, N.J. Dudney, B. Neudecker, A. Ueda, C.D. Evans, Solid State Ionics 135 (2000) 33–45.
[3] F. Beck, P. Hulser, J. Electroanal. Chem. 280 (1990) 159–166.
[4] K. Naoi, M. Takeda, H. Kanno, M. Sakakura, A. Shimada, Electrochim. Acta 45 (2000) 3413–3421.
[5] S. Niwa, Y. Taketani, J. Power Sources 60 (1996) 165–171.
[6] S. Tsuchiya, Y. Kudoh, T. Kojima, M. Fukuyama, S. Yoshimura, EP 336,299 (1989).
[7] J.S. Do, S.H. Yu, S.F. Cheng, J. Power Source 112 (2003) 203–211.
[8] P.H. Humble, J.N. Harb, R. LaFollette, J. Electrochem. Soc. 148 (2001) A1357–A1361.
[9] D.M. Cheseldine, US Patent 4,164,005 (1979).
[10] M. Nathan, E. Peled, D. Haronian, US Patent 6,197,450 (2001).
[11] M. Tanahashi, M. Shimada, E. Igaki, Four-terminal capacitor, EP 936,642 (1999).
[12] H. Yamamoto, M. Oshima, T. Hosaka, I. Isa, Synth. Met. 104 (1999) 33–38.
[13] Y. Itoh, S. Yashimura, J. Electrochem. Soc. 124 (1977) 1128–1133.
[14] J. Kyokane, K. Yoshino, Synth. Met. 55–57 (1993) 3774–3779.
[15] T. Nishiyama, K. Sakata, T. Fukaumi, A. Kobayashi, S. Arai, US Patent 5,428,500 (1995).
[16] S. Niwa, Synth. Met. 18 (1987) 665–670.
[17] A. Yoshida, A. Nishino, US Patent 4,046,6451 (1977).
[18] K. Amano, H. Ishikawa, E. Gasegawa, US Patent 5,586,001 (1996).
[19] M. Fukuda, H. Yamamoto, I. Isa, EP Patent 274,755 (1988).
[20] Y. Harakawa, K. Izawa, H. Takeuchi, S. Nakamura, S. Toita, EP Patent 283,239 (1988).
[21] Y. Harakawa, K. Izawa, H. Takeuchi, S. Nakamura, S. Toita, EP Patent 285,728 (1988).
[22] A. Kobayashi, H. Yageta, T. Date, T. Fukaumi, US Patent 5,951,721 (1999).
[23] A. Kobayashi, T. Fukaumi, K. Amano, H. Ishikawa, M. Satoh, US Patent 5,959,832 (1999).
[24] L.H.M. Krings, E.E. Havinga, J.J.T.M. Donkers, F.T.A. Vork, Synth. Met. 54 (1993) 453–459.
[25] Y. Kudoh, S. Tsuchiya, T. Kojima, M. Fukuyama, S. Yoshimura, Synth. Met. 41–43 (1991) 1133–1136.
[26] Y. Kudoh, M. Fukuyama, S. Yoshimura, Synth. Met. 66 (1994) 157–164.
[27] Y. Kudoh, T. Kolima, M. Fukuyama, S. Tsuchiya, S. Yoshimura, J. Power Source 60 (1996) 157–163.
[28] Y. Kudoh, K. Akami, Y. Matsuya, Synth. Met. 102 (1999) 973–974.
[29] J. Li, J.Z. Zhang, Y.H. Geng, L.X. Wang, X.B. Jing, F.S. Wang, Synth. Met. 69 (1995) 245–246.
[30] B.J. Melody, J.T. Kinard, P.M. Lessner, US Patent 5,853,794 (1998).
[31] K. Naoi, Y. Oura, A. Yoshizawa, M. Takeda, M. Ue, Electrochem. Solid-State Lett. 1 (1998) 34–36.
[32] A. Nishino, H. Kumano, H. Hayakawa, US Patent 3,801,479 (1974).
[33] K.S. Park, Y.J. Park, M.K. Kim, J.T. Son, H.G. Kim, S.J. Kim, J. Power Sources 103 (2001) 67–71.
[34] S.D. Ross, W. Mass, US Patent 5,223,002 (1993).
[35] M. Satoh, H. Ishikawa, K. Amano, E. Hasegawa, K. Yoshino, Synth. Met. 71 (1995) 2259–2260.
[36] R. Taylor, H.E. Haring, J. Electrochem. Soc. 103 (1956) 611–613.
[37] L.C. Thompson, C. Li, K.K. Lian, US Patent 5,826,729 (1997).
[38] W.C. West, J.F. Whitacre, V. White, B.V. Ratnakumar, J. Micromech. Microeng. 12 (2002) 58–62.
[39] M.S. Yun, C.S. Huh, Synth. Met. 28 (1989) C715–C721.
[40] F. Larmat, J.R. Reynolds, Y.J. Qiu, Synth. Met. 79 (1996) 229–233.
[41] J.S. Shaffer, EP Patent 135,223 (1985).
[42] H. Yamamoto, M. Fukuda, I. Isa, Electron. Commun. Jpn. 76 (1993) 745–753.
[43] M. Satoh, H. Ishikawa, K. Amano, E. Hasegawa, K. Yoshino, Synth. Met. 65 (1994) 39–44.
[44] F. Beck, P. Hulser, R. Michaelis, Bull. Electrochem. 8 (1992) 35–44.
[45] K.M. Cheung, D. Bloor, G.C. Stevens, Polymer 29 (1988) 1709–1717.
[46] P. Hulser, F. Beck, J. Electrochem. Soc. 137 (1990) 2067–2069.
[47] P. Hulser, F. Beck, J. Appl. Electrochem. 20 (1990) 596–605.
[48] D.A. Jones, second ed., Prentice Hall, Upper Saddle Rive, 1996, p. 56.
[49] J.F. Moulder, W.F. Strickle, P.E. Sobol, K.D. Bomben, Handbook of X-ray Photoelectron Spectroscopy, Perkin–Elmer, Eden Prairie, 1995.
[50] T. Endo, K. Kubo, S. Hiyama, FUJITSU Sci. Tech. J. 5 (1969) 87–116.